

Radiation emission of autoionising hole states of Al induced by XUV free electron laser radiation with FLASH at DESY

E. Galtier^{1*}, F.B. Rosmej^{1,2†}, D. Riley³, T. Dzelzainis³, P. Heinmann⁴,
FY. Khattak³, R.W. Lee⁴, B. Nagler⁵, A. Nelson⁴, T. Tschentscher⁶,
S.M. Vinko⁵, T. Whitcher⁵, S. Toleikis⁶, R. Fäustlin⁶, L. Juha⁷,
M. Fajardo⁹, J.S. Wark⁵, J. Chalupsky⁷, V. Hajkova⁷, J. Krzywinski⁸,
R. Soberierski¹⁰, M. Jurek¹⁰, M. Kozlova⁷

¹*Université Pierre et Marie Curie, LULI, UMR 7605, case 128, 75252 Paris Cedex 05, France*

²*Ecole Polytechnique, LULI, PAPD, 91128 Palaiseau, France*

³*School of Mathematics and Physics, Queen's University Belfast, Belfast BT7 1NN, UK*

⁴*Lawrence Livermore National Laboratory, USA*

⁵*Clarendon Laboratory, University of Oxford, South Parks Road OX1 3PU, UK*

⁶*HASYLAB DESY, Hamburg*

⁷*Institute of Physics, AS CR, Prague 8*

⁸*SLAC, Menlo Park CA, USA*

⁹*Instituto Superior Técnico, U. Técnica de Lisboa*

¹⁰*Inst. of Physics, Polish Academy of Sciences*

Abstract

The analysis of the radiative properties of plasmas created by XUV and X-ray free electron laser radiations provides a tremendous challenge to researchers to investigate matter under extreme conditions. In the present work we report about the theoretical analysis of the radiation emission of Al heated by the interaction of 10 fs focused ($1 \mu\text{m}$) free electron laser radiation at 13.5 nm at intensities of about 10^{16} W/cm^2 . The data show strong resonance line emission $3l - 2l'$ from Ne-like Al but also numerous intense broad emission structures in the spectral range from 10 – 30 nm. Atomic structure analysis indicate that these emission structures might originate from multiple excited states with L-holes. By means of a genetic algorithm we analyze possible excitation channels driven directly by the FLASH free electron laser as well as by heated plasma electrons.

*eric.galtier@upmc.fr

†frank.rosmej@upmc.fr

Experimental setup

The XUV free electron laser located at Ham-bourg, Germany, has been used at the wavelength of 13.5 nm , with a mean energy per pulse of about $5 - 10 \mu\text{J}$ at 5 Hz . A 3 mm aperture has been used before the entrance of the chamber in order to limit the size of the beam. In a high vacuum chamber (10^{-6} torr), a micro-focusing off-axis parabola, coated with a multi-layer of $\text{Mo} - \text{Si}$ having a focal length of 269 mm , allowed us to get a focal spot size of $1.5 \mu\text{m}$. As the pulse duration of FLASH beam is 15 fs we have reached an intensity of about 10^{16} W/cm^2 . Thus, the interaction of the FEL with an aluminium foil ($Z = 13$) created a plasma whose emission has been dispersed in the range of $10 - 30 \text{ nm}$ using a Hitachi variable line spacing grating ($\sim 1200 \text{ lines/mm}$) and recorded with an Andor DX420 – BN CCD camera. The aluminium foil was $10 \mu\text{m}$ thick and translated perpendicularly to the beam in order to expose a fresh area to each set of pulses. The analysed spectra accumulate 2000 shots in order to enhance the contrast (the CCD was set at -10°C). Figure 1 illustrates the inner chamber configuration.

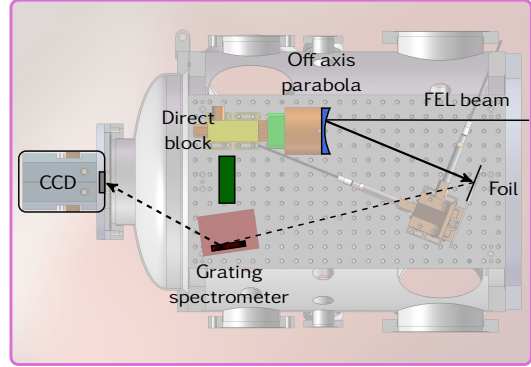


Figure 1: Top view of the experimental setup.

Numerical approach

The black curve in the figure 2 shows the observed spectrum. The strong emissions at ~ 13 and 16 nm correspond to Neon-like transitions $\text{Al IV } (3l' \rightarrow 2l)$ given by a Hartree – Fock code [1]. Other numerous transitions are observed on the red wings of these lines. Their origin will be discussed in detail in the next section. In order to investigate possible excitation channels to explain these wings we approximate the experimental spectral distribution function by $I(\omega) = \sum_k f_k \sum_i \sum_j \hbar \omega_{ji} \cdot g_j A_{ji}^k \cdot \phi_{ji}^k(\omega_{ji} + \Delta\omega_k) \cdot e^{\frac{-E_j}{k_B T}}$ (1), where f_k is a weight for each configuration and $\Delta\omega_k$ is a wavelength shift. These are free parameters for the genetic algorithm described in the flow diagram of figure 3. The main idea is to use possible configurations describing the data and mix them together in order to better describe the experimental spectrum (in particular the red line wings). This mixing procedure has been divided into two different steps. The first one consists in the computation of the transition wavelengths, the energy levels, the statistical weight and radiative decay rate using a Multi Configuration Hartree – Fock code (MCHF) in intermediate coupling approach. Then the associated spectral distribution and line shapes (including radiation transport) are determined using the MARIA code [3, 4]. This first step is the *pre processing* and takes most of the computation time of the whole numerical procedure. Then,

we take each spectral distributions in order to mix them into a genetic algorithm [2] to describe the data. We have modified the existing version to operate in double precision and to accept as many configurations as needed.

The goal of such evolutionary algorithm is to be robust under possible premature convergence independently of the complexity of the problem. Indeed, in our case, we have set as free parameters a wavelength shift and the intensity for the three configurations involved, as well as two parameters for a linear background : 8 parameters had to be handled by the algorithm. What the genetic algorithm does first is to evaluate each configuration with a random value assigned to each free parameters (this is the first population at the first generation). Then a sum over the in-

tensity of the linear background and each configuration is performed giving a first *random* overall spectrum. To estimate how this spectrum corresponds to the experimental one, a fitness function is used : we have chosen a square law for a direct evaluation of the goodness of the fit, $\xi^2 = |I_{exp}(\lambda) - I_{th}(\lambda)|^2$. Then, the genetic algorithm will maximize the inverse of this number for each step of the algorithm (or generation) : a small ξ^2 will corresponds to a small discrepancy between experiment and theory, as well as a big inverse ξ^2 . At the end of each step, a selection of the new child that corresponds to the highest similarity with the experimental spectrum is done, preceding the crossover and mutation operations on the parameter sequence (parent) that breed the population of parameters and create new (better or worth) values for the free parameters. After a user fixed number of generation the algorithm will stop and provide the set of parameters that corresponds to the fittest spectrum.

Results and discussion

The red curve in the figure 2 is the result of this procedure : the spectrale distribution (eq. 1) of all line transitions originating from the configurations $K^2L^7M^1$ have been calculated for $kT_e = 8 eV$, whereas those from $K^2L^7M^2$ and $K^2L^7M^3$ configurations have been calculated for $kT_e = 25 eV$. Emission from $K^2L^7M^2$ and $K^2L^7M^3$ configurations corresponds to a plasma created right after the destruction of the aliminium lattice. Indeed, the time evolution of the laser XUV - matter interaction is described as follows : first, the laser create holes by direct photoionisation

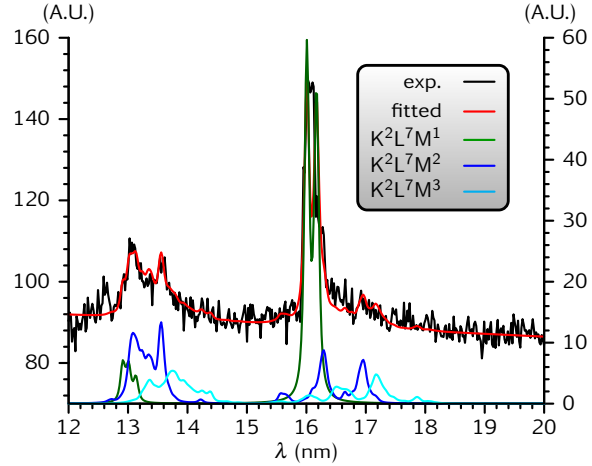


Figure 2: Good agreement between fit and experiment.

($h\nu_{FEL} = 92.5 \text{ eV}$) of the neutral aluminium L shell because of a higher photionisation cross section for inner shells than outer shells ($\sigma_{PI} \sim E_I^{5/2}$ with $E_I^L > E_I^M$). A very fast 3 body recombination regime ($K^2L^7M^3 + 2e^-$) follows creating $K^2L^7M^4$.

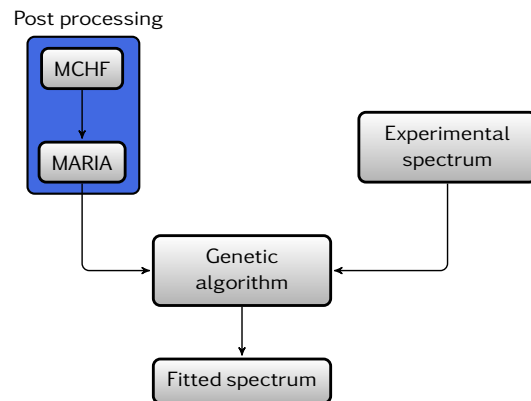


Figure 3: Numerical procedure used to analyse the spectra.

Then usually metal fluorescence takes place. At this same time, autoionisation processes take place because aluminium is multiply excited. This short time scale for desexcitation ($\tau_{AI} \sim \frac{1}{A+\Gamma} \sim 40 - 100 \text{ fs}$) provides an Auger electron to the continuum with a kinetic energy of about 60 – 80 eV immediately after the laser pulse. Because of the high intensity, a saturated absorption regime has been reached [5] allowing almost all $2p^6$ electrons to participate as an Auger electron. Rapid redistribution (1 fs) between the existing "cold" M electrons may lead to a electron temperature of about 20 eV. Then,

an electron – phonon coupling takes place, and on a time scale of 1 ps [6] after the laser interaction, the aluminium lattice will start to collapse (solid – atomic transition phase behaviour). Now, a dense coupled plasma (WDM) is created allowing ionisation of M shell electrons. These ionised states give rise to dielectronic capture followed by dielectronic recombination on a few hundred femtosecond time scale. The observed transitions correspond therefore most probably to this dielectronic recombination regime. As a consequence, the genetic algorithm analysed the *early* life time of the warm and dense created plasma.

References

- [1] R.D. Cowan, The Theory of Atomic Structure, Berkeley (1980).
- [2] P. Charbonneau and B. Knapp, A User's guide to PIKAIA 1.0, NCAR Technical Note 418+IA (Boulder: National Center for Atmospheric Research) (1995).
- [3] Rosmej F.B., J. Phys. B Lett.: At. Mol. Opt. Phys. 30 (1997) L819.
- [4] Rosmej F.B., Europhysics Letters 76 (2006) 1081.
- [5] Nagler B. et al, Turning solid aluminium transparent by intense soft x-ray photo-ionisation, Nature Physics (2009).
- [6] Lin Zhibin and Zhigilei Leonid V., Electron-phonon coupling and electron heat capacity of metals under conditions of strong electron-phonon nonequilibrium, PRB (2008).